Reservoirs & fluxes of H_2O on the Earth

The hydrological cycle (Berner)

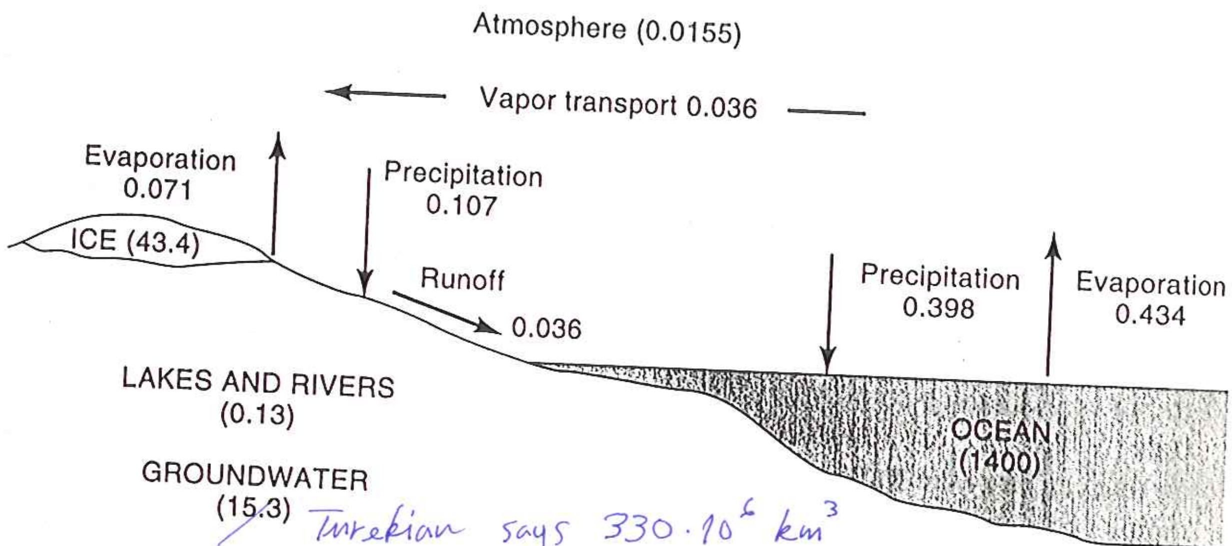

Figure 1.1 The hydrologic cycle. Numbers in parentheses represent inventories (in 10^6 km^3 = 10^{18} kg) for each reservoir. Fluxes are in 10^6 km^3/yr (10^{18} kg/yr). (Data from Table 1.1 and NRC 1986.)

The fluxes between the reservoirs are measured in 10^6 km^3/yr = 10^{18} kg/yr.

Can convert to an equivalent rainfall rate, averaged over the ⊕'s surface:

$$\frac{10^6 \text{ km}^3/\text{yr}}{4\pi\,(6371 \text{ km})^2} = 2 \cdot 10^{-3} \frac{\text{km}}{\text{yr}} = 2000 \frac{\text{mm}}{\text{yr}}$$

So, we multiply by 2000 to get Berner's fluxes in mm/yr of equivalent rainfall.

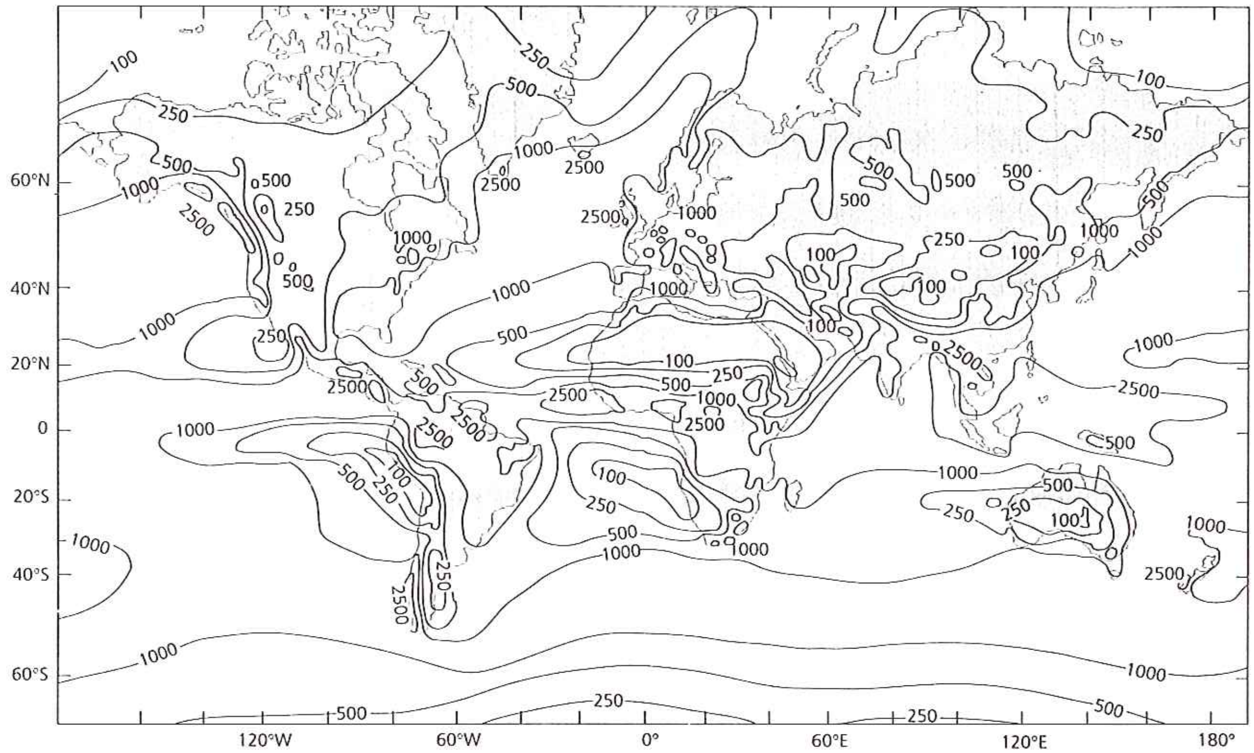

Fig. 1.17 The geographical variation of mean annual precipitation, in millimetres. After Lamb (1972) [19].

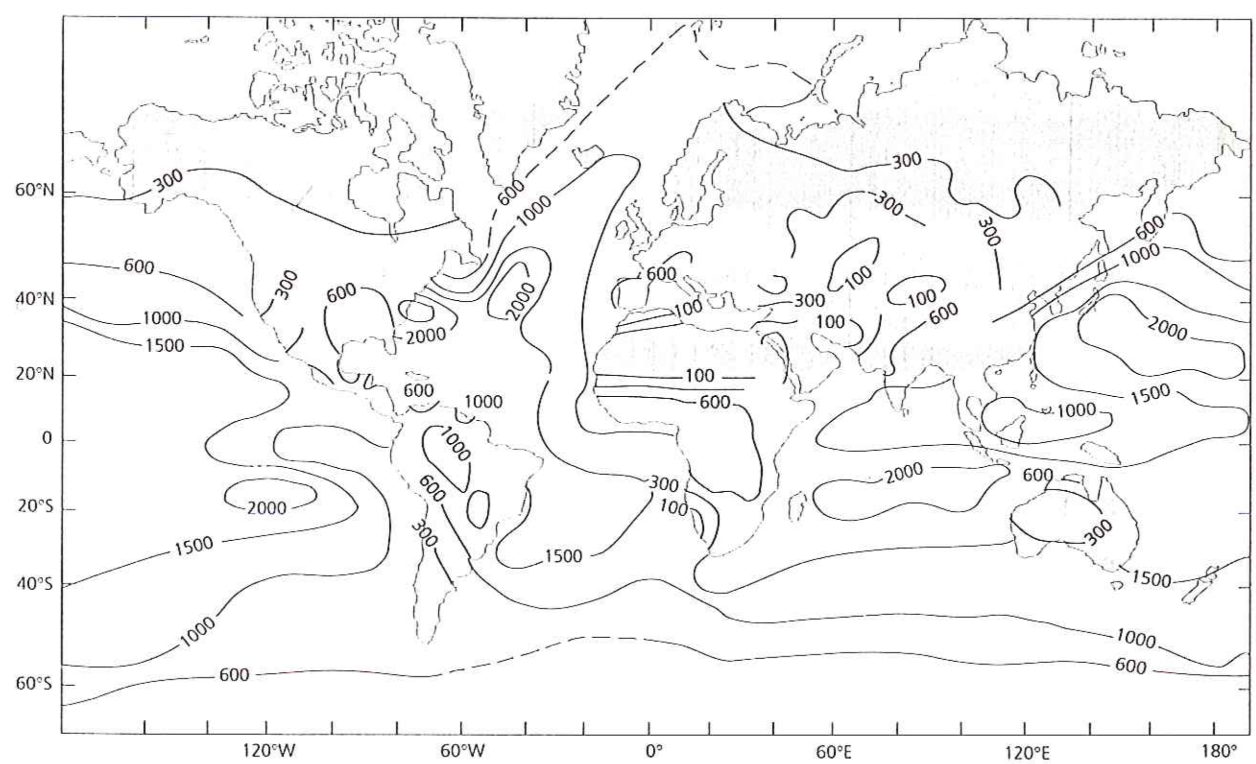

Fig. 1.18 Geographical variation of annual evaporation from ocean and evapotranspiration from land surface, in millimetres. After Barry (1970) [20].

Steady-state box models:

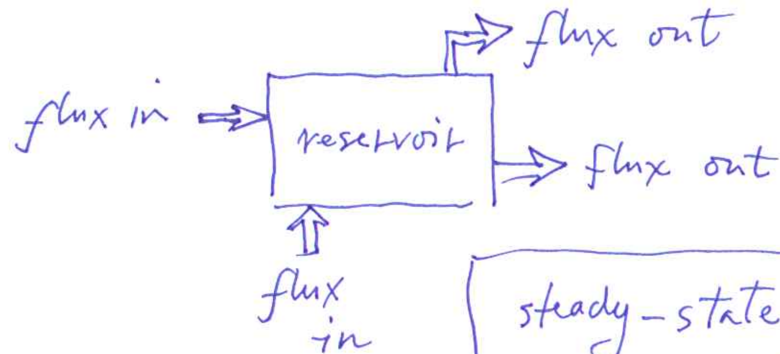

steady-state condition:
$\sum$ fluxes in = $\sum$ fluxes out

Example:
ocean-to-continent H_2O vapor transport is balanced by stream runoff

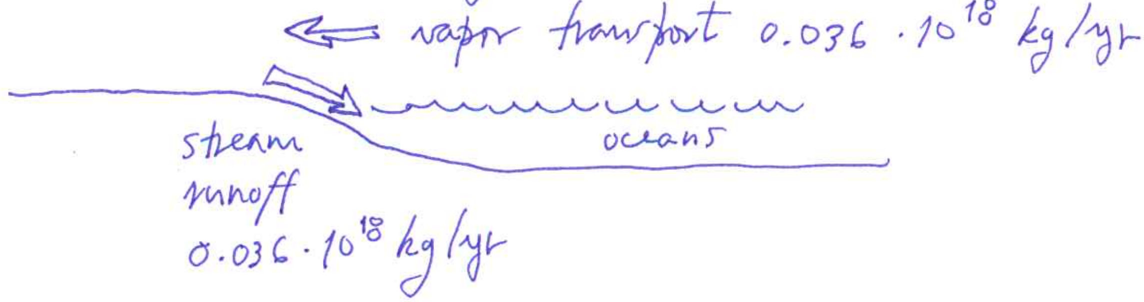

Concept of residence time: example – Princeton students

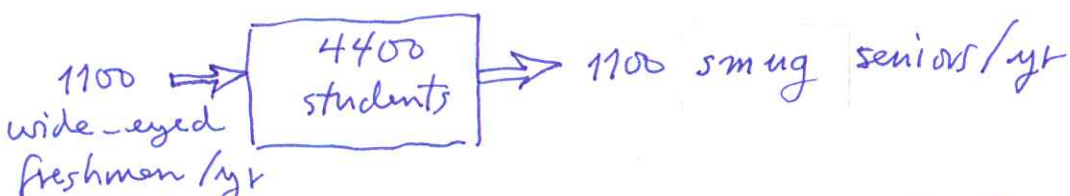

residence time of a student in the "reservoir"

$$\frac{4400 \text{ students}}{1100 \text{ students/yr}} = 4 \text{ years!}$$

Residence time of an H_2O molecule in the atmosphere:

$$\underset{\substack{\text{continental}\\\text{rainfall}}}{\frac{0.155 \cdot 10^{18}\ kg}{(0.107 + 0.398) \cdot 10^{18}\ kg/yr}} = 0.03\ yr = \underline{11\ days}$$

continental rainfall — oceanic rainfall

This is the typical time between major rainstorms.

Residence time of an H_2O molecule in the oceans:

$$\frac{1400 \cdot 10^{18}\ kg}{(0.398 + 0.036) \cdot 10^{18}\ kg/yr} = \underline{3000\ years}$$

oceanic rainfall — river runoff

Since the oceans dominate the mobile H_2O reservoir, this can be thought of as the homogenization time for this reservoir.

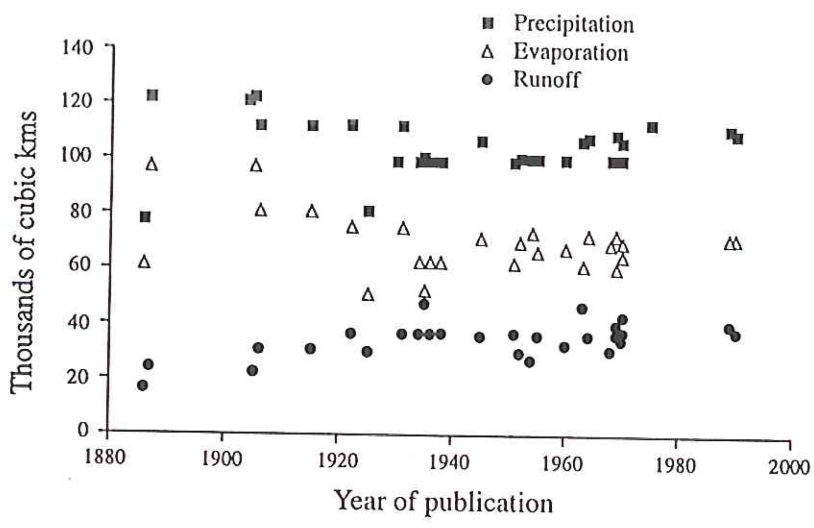

Figure 4.14 Scattergraph of various estimates of the three main components of the Global Water Balance from 1880 to 1995 (data mostly from Baumgartner and Reichel, 1975)

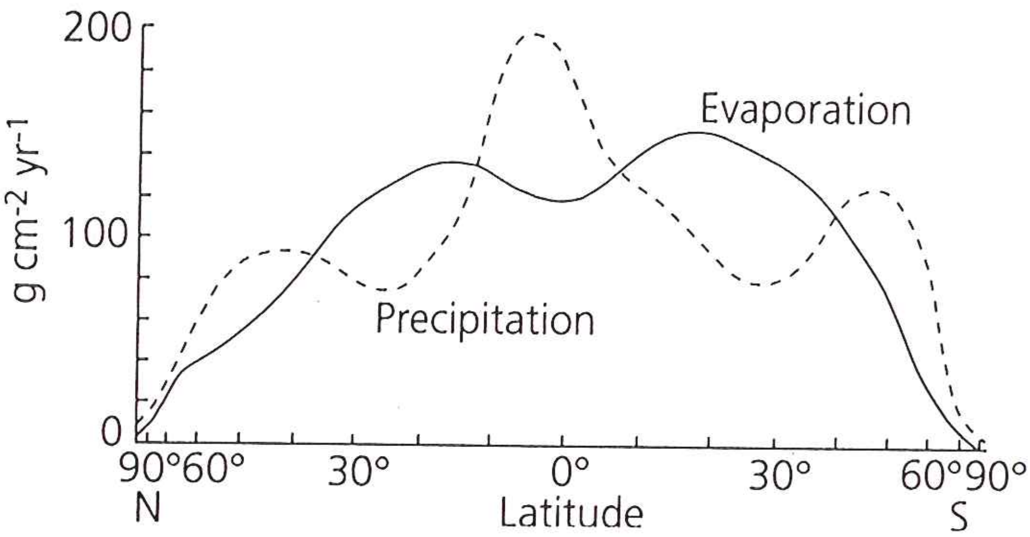

Fig. 1.19 Zonally averaged precipitation and evaporation as a function of latitude.

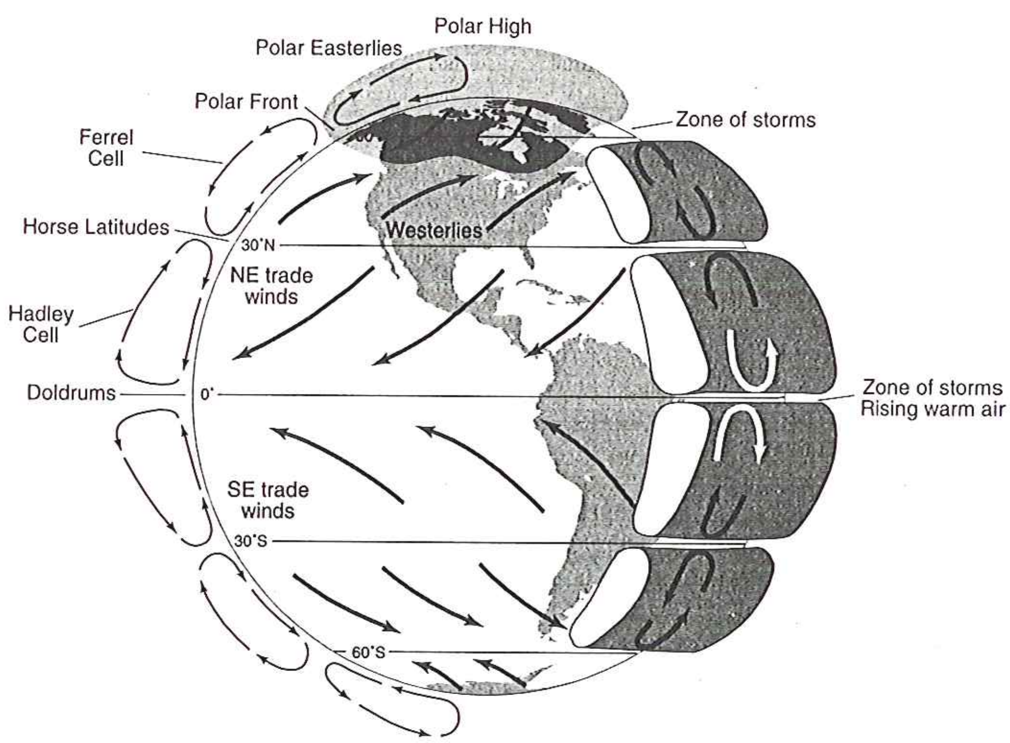

Figure 1.9 Schematic representation of the general circulation of the atmosphere. (Frederick K. Lutgens/Edward J. Tarbuck, *The Atmosphere*, 5th ed., Copyright © 1992, p. 170. Adapted by permission of Prentice Hall, Englewood Cliffs, New Jersey.)

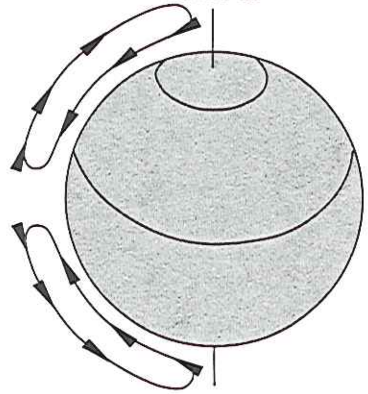

Figure 6.3 On a nonrotating planet, air that rises in low latitudes flows poleward aloft, sinks in high latitudes, and returns equatorward near the surface.

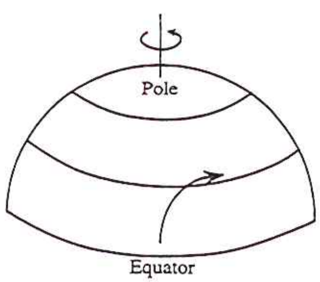

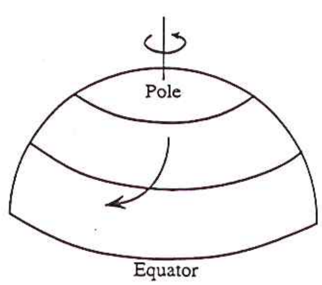

Figure 6.4 *Left,* Parcels of air in low latitudes are initially far from Earth's axis of rotation and therefore are moving rapidly eastward. When they move poleward and retain their angular momentum, they move eastward relative to Earth's surface beneath them. *Right,* Equatorward-moving parcels, on the other hand, move westward relative to the surface beneath them.

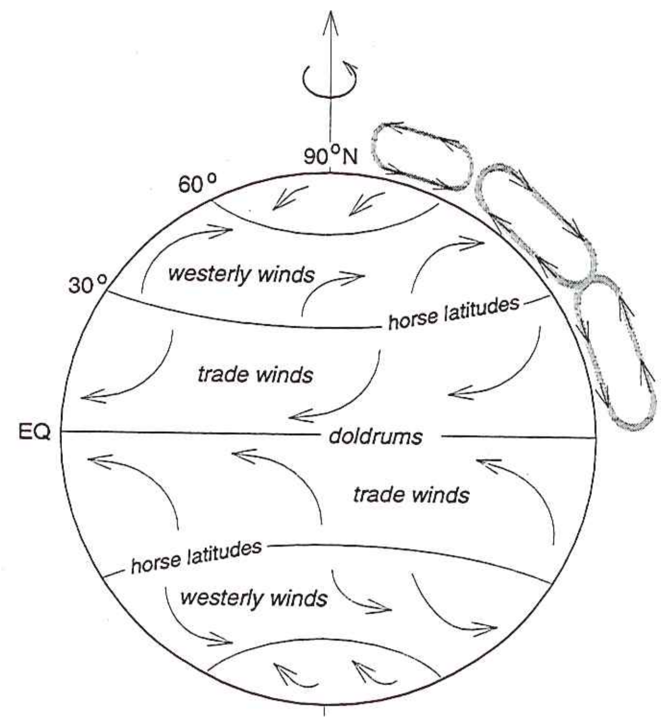

Figure 6.6 The southeast and northeast trade winds in the tropics converge onto the doldrums, rainy regions where moist air rises. In the subtropics, the easterly and westerly winds diverge from the horse latitudes, sunny, dry regions over which dry air subsides. The easterly winds in polar regions, and the westerlies in subpolar regions, converge onto rainy regions near 60°N and 60°S, respectively.

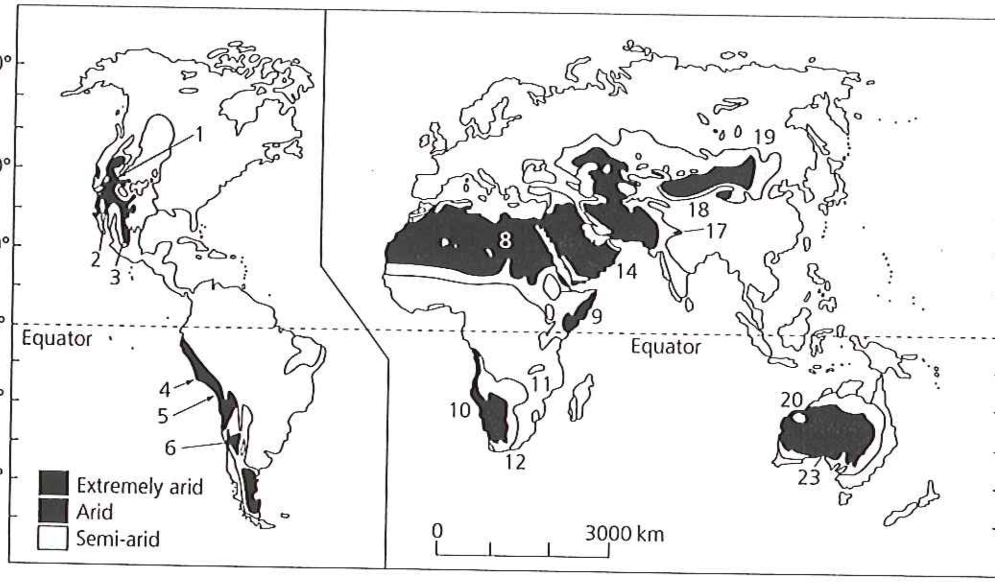

Fig. 10.24 Distribution of the world's drylands. The main deserts are: (1) Great Basin; (2) Sonoran; (3) Chihuahuan; (4) Peruvian; (5) Atacama; (6) Monte; (7) Patagonian; (8) Sahara; (9) Somali-Chabli; (10) Namib; (11) Kalahari; (12) Karroo; (13) Arabian; (14) Rub al Khali; (15) Turkistan; (16) Iranian; (17) Thar; (18) Taklimakan; (19) Gobi; (20) Great Sandy; (21) Simpson; (22) Gibson; (23) Great Victoria; (24) Sturt. After Cooke & Warren (1973) [32] and Greeley & Iversen (1985) [9].

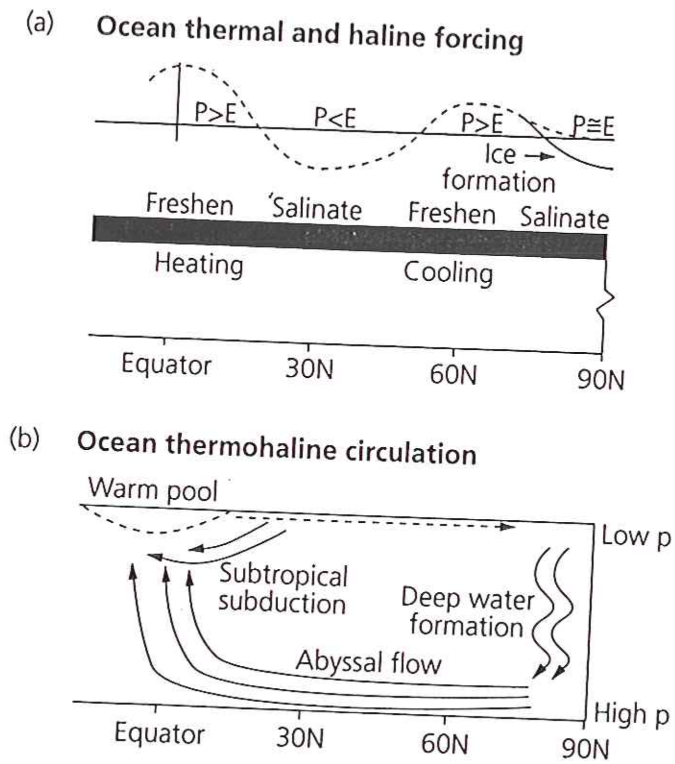

Fig. 1.7 Forcing mechanisms and circulation in the ocean. (a) Thermal and haline forcing. (b) Resulting thermohaline oceanic circulation (P = pressure). After Webster (1994) [7].

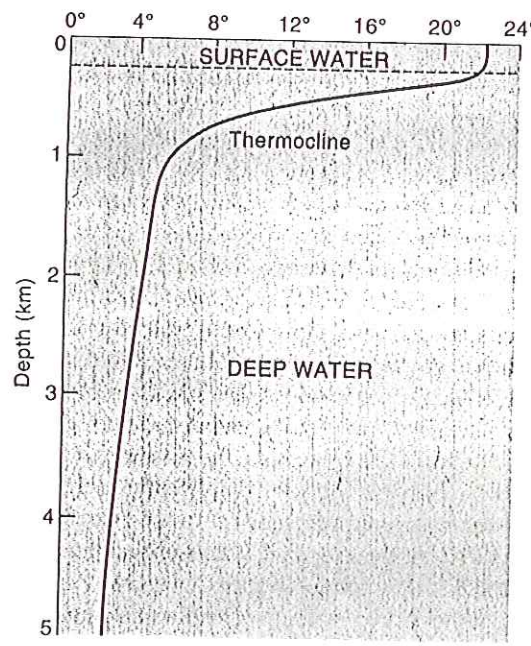

Ocean homogenization time ~ 1000 yrs

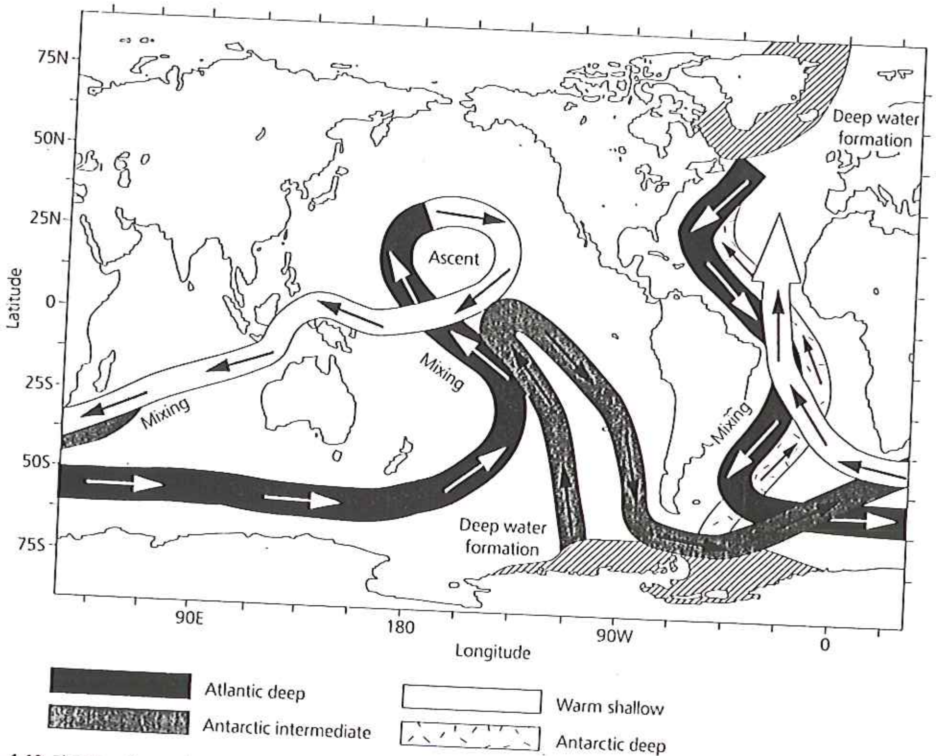

Fig. 1.10 The deep thermohaline circulation of the oceans, modified from Stommel (1958) [12]. The major sources of deep water at the present day in the north Atlantic and Weddell Sea are shown by hatching. The lack of deep water formation in the north Pacific may be due to the greater stability of the Pacific caused by the higher fresh water flux. The text describes the circulation patterns observed.

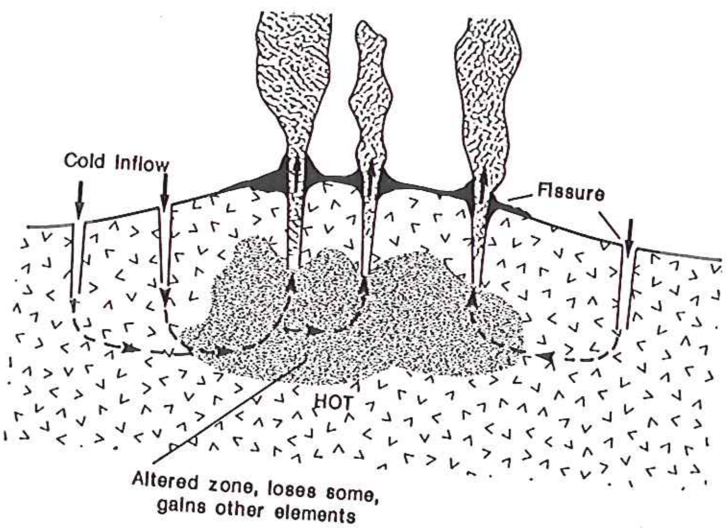

Figure 14.3. The hot crust of the mid-ocean ridges is cooled partly by conduction of heat to the seafloor. Almost as much heat is carried away by cold ocean water that enters fissures and circulates through the hot crust. Once heated, the water returns to the ocean as hotsprings, with exit temperatures that range from a few degrees to 350 °C. While passing through the hot crust the seawater leaves some constituents behind and extracts others, thereby altering the rocks substantially. At the vents, manganese and iron oxides and hydroxides (black) are deposited that may contain valuable amounts of such metals as silver and copper.

not boiling because of high pressure

Time required to cycle the entire ocean through the hot basaltic crust:

$$\frac{\text{volume of oceans}}{\text{flux of all hot springs}} = \frac{1400 \cdot 10^6 \text{ km}^3}{200 \text{ km}^3/\text{yr}} = 7 \text{ Myr}$$

200 km³/yr ← $\frac{1}{3}$ flow of Mississippi at mouth